

# Collective Quantum Behavior of Electron–Phonon Condensates

John H. Miller, Jr.,<sup>1,3,\*</sup> Jayahansa Napagoda,<sup>1,3</sup> Asanga I. Wijesinghe,<sup>4</sup> Martha Y. Suárez – Villagrán,<sup>1,3</sup> Jarek Wosik,<sup>2,3</sup> & Byron Freelon<sup>1,3</sup>



UNIVERSITY OF  
HOUSTON

1) Dept. of Physics, University of Houston; 2) Dept. of Electrical & Computer Engineering, University of Houston;  
3) Texas Center for Superconductivity at the University of Houston; 4) Tetra Tech, Inc., Houston, Texas.

\* jhmiller@uh.edu.

Texas Quantum Summit, Texas A&M University, September 19-20, 2025

## Introduction

The charge density wave (CDW) is a correlated electron–phonon condensate that forms in 2D and quasi-1D materials. For temperatures ranging up to well above room temperature, current-voltage plots of various trichalcogenides agree with our quantum simulations of CDW transport [1, 2]. Our model treats the Schrödinger equation as an emergent ‘classical’ equation describing Josephson-like coupling between macrostates, viewed as thermally robust complex order parameters.

Quantum behavior is further revealed by oscillations of period  $h/2e$  in CDW conductance vs. magnetic flux in 85- $\mu\text{m}$  circumference  $\text{TaS}_3$  rings above 77 K [3]. While compelling, CDW rings are difficult to grow reproducibly, so it is desirable to reveal some form of quantum phase coherence that can be observed in ordinary single crystals and, ultimately, patterned thin films.

## Approach

**Temporal modulation of quantum phase.** The ac Josephson effect in a superconducting tunnel junction is perhaps the best-known example involving temporal modulation of quantum phase between macroscopic wavefunctions (complex order parameters). We have begun a series of experiments where quantum phase becomes modulated between coupled macrostates in CDWs.

The relative quantum phases of the macrostates in our model [1, 2] can be modulated by an oscillatory electric field. This is related to the scalar Aharonov-Bohm effect, where a time-varying scalar potential couples to quantum mechanical phase. The theory of photon-assisted tunneling [4] enables predictions of response to combined dc and ac signals based on the system’s I-V characteristic. The basic idea is that oscillatory voltages temporally modulate the energies and relative phases between coupled macrostates, which leads to Bessel-type behavior when plotted vs. amplitude.

The approach discussed here entails harmonic mixing, where one applies a signal of the form,  $V(t) = V_1 \cos \omega_1 t + V_2 \cos \omega_2 t$ , and (e.g., using a lock-in amplifier) measures the induced response:  $\delta I(t) = \delta I_0 \cos(\omega_0 t + \varphi)$ , where  $\omega_0 = |\omega_2 - 2\omega_1|$ . This is measured in the presence of a large-amplitude ac ‘bias’ voltage  $V_{ac} \cos \omega t$ . The harmonic mixing response  $\delta I_0$  is then plotted vs. amplitude,  $V_{ac}$ . The normalized theoretical response can be approximated as:

$$\frac{\delta I_0}{\delta I_m} \cong J_0^2 \left( \frac{V_{ac}}{\alpha \omega} \right) + \sum_{n=1}^N A_n(\omega) J_n^2 \left( \frac{V_{ac}}{\alpha \omega} \right). \quad (1)$$

Using  $V_{ac} = (L/\ell)V_\ell$ , where  $L$  is the distance between contacts,  $\ell$  is an effective distance for Josephson-like tunneling of electron pairs, and taking the effective charge to be  $2e$ , one obtains the following scaling parameter:

$$\alpha = \frac{L \hbar}{\ell 2e}. \quad (2)$$

## Results

Figures 1 and 2 show examples, where harmonic mixing response (involving two input signals) of the CDW in  $\text{TaS}_3$  or  $\text{NbSe}_3$  is plotted vs. the amplitude of a third, larger amplitude signal at various frequencies. Note the Bessel-type behavior, where the spacing increases with frequency. The results suggest that  $\text{TaS}_3$  shows greater quantum coherence than  $\text{NbSe}_3$ .

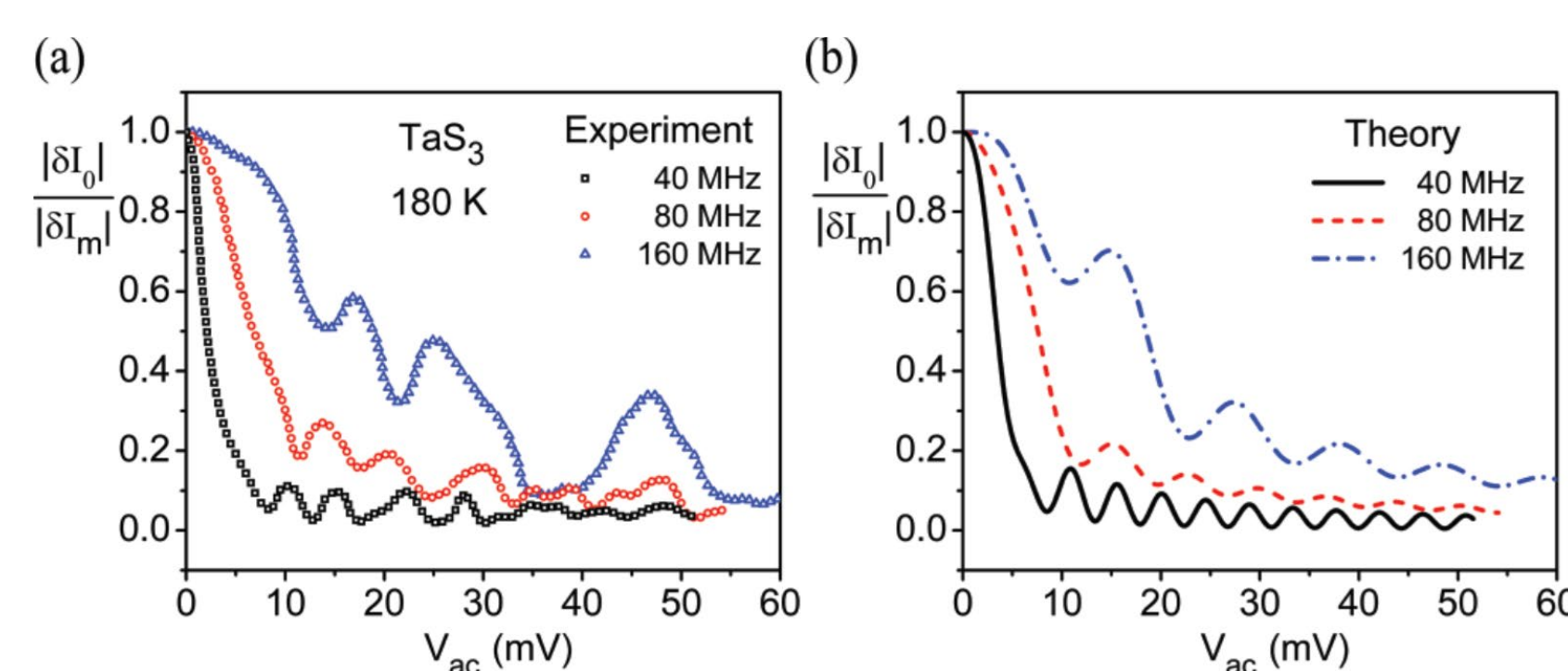


**Fig. 1. (a)** Normalized magnitude of harmonic mixing response ( $\omega_1/2\pi = 5$  MHz,  $\omega_2/2\pi = 14$  MHz,  $\omega_0/2\pi = 4$  MHz) of a 0.1-mm-long  $\text{TaS}_3$  crystal vs ac bias amplitude  $V_{ac}$  at three different frequencies  $\omega/2\pi$  at 180 K. **(b)** Theoretical plots using sums of Bessel functions, Eq. (1), and the parameters in Table I.

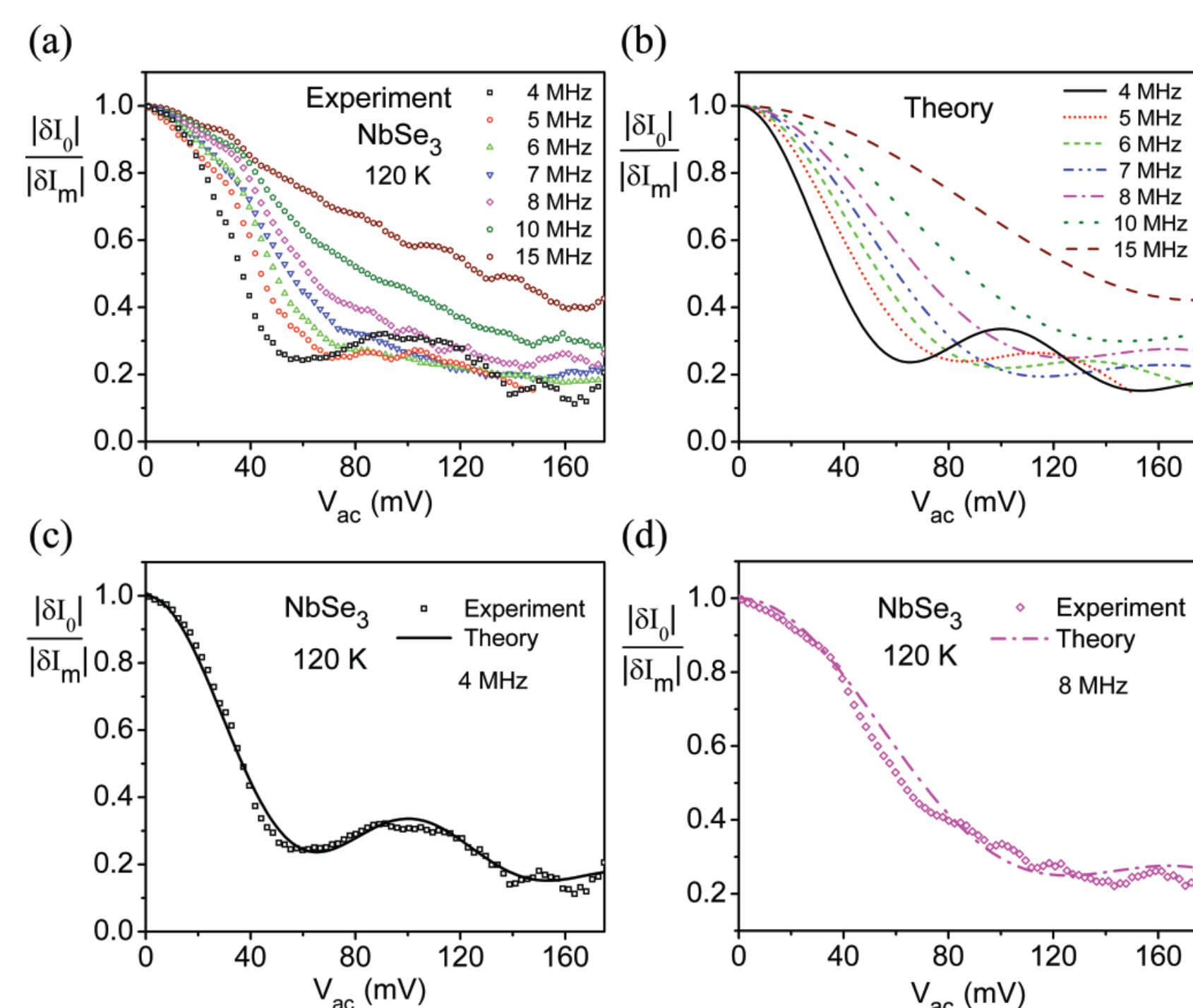


**Fig. 2. (a)** Normalized magnitude of harmonic mixing response ( $\omega_1/2\pi = 1$  MHz,  $\omega_2/2\pi = 2.8$  MHz,  $\omega_0/2\pi = 800$  kHz) of an  $\text{NbSe}_3$  crystal ( $L = 5$  mm), vs ac bias amplitude  $V_{ac}$  at several frequencies  $\omega/2\pi$  at 120 K. **(b)** Theoretical plots using Eq. (1) and the parameters shown in Table II. **(c)** and **(d)** Direct comparisons between theory and experiment for frequencies  $\omega/2\pi$  of 4 MHz and 8 MHz.

TABLE I. Eq. (1) parameters used for the Fig. 1 theoretical plots.

| $\omega/2\pi$ (MHz) | $\alpha$ (V·s)        | $A_1$ | $A_2$ | $A_3$ | $A_4$ |
|---------------------|-----------------------|-------|-------|-------|-------|
| 40                  | $5.5 \times 10^{-12}$ | 1.75  | 0.25  | 0.42  | -1.00 |
| 80                  | $4.2 \times 10^{-12}$ | 1.80  | 1.40  | 0.50  | -0.60 |
| 160                 | $3.2 \times 10^{-12}$ | 2.00  | 0.70  | 1.57  | 1.44  |

TABLE II. Eq. (1) parameters used for the Fig. 2 theoretical plots.

| $\alpha = 1.1 \times 10^{-9}$ (V·s) | $A_1$ | $A_2$ | $A_3$ | $A_4$ |
|-------------------------------------|-------|-------|-------|-------|
| 4 MHz                               | 0.40  | 0.65  | 0.15  | 0.55  |
| 5 MHz                               | 0.45  | 0.70  | -0.30 | 0.10  |
| 6 MHz                               | 0.30  | 1.00  | -1.40 | 1.90  |
| 7 MHz                               | 0.20  | 1.10  | -2.00 | 3.50  |
| 8 MHz                               | 0.20  | 1.40  | -1.65 | 0.70  |
| 10 MHz                              | 0.15  | 1.90  | -1.90 | -1.95 |
| 15 MHz                              | 0.01  | 3.00  | 3.00  | 1.00  |

## Future Directions

New versions of our quantum phase modulation experiments are currently in progress. We also plan discussions with nanolithography companies to explore patterning of epitaxial dichalcogenide films.

Longer-term, potential applications of electron-phonon condensates, such as CDWs, include quantum reservoir computing [2], where a 2D material ‘reservoir’ between input and output neural network layers enhances learning speed.

For circuit-based quantum computing, hybrid devices [5, 6] could be tested. In one version a superconductor coupled to a CDW or quantum paraelectric acts as a nonlinear LC resonator, like a transmon in which the roles of linear and nonlinear elements are reversed. Experiments could look for signatures, such as Rabi oscillations, at higher-than-mK temperatures due to macroscopic occupation of phasons or phonons.

Additional approaches might explore various forms of quantum annealing or continuous variable quantum computing, which may hold potential for dissipative quantum systems such as the ones we discuss here.

The most compelling argument for supporting new research on thermally robust quantum systems is the fact that mK-cooled quantum computers are, at best, large and extremely expensive, and may prove difficult to scale for practical applications.

## References

1. Miller Jr., J. H., Suárez-Villagrán, M. Y., & J.O. Sanderson, J. O. Quantum transport of charge density wave electrons in layered materials. *Materials Today Phys.* **41**, 101326 (2024).
2. Miller Jr, J. H. & Suárez-Villagrán, M. Quantum fluidic charge density wave transport. *Appl. Phys. Lett.* **118**, 184002 (2021).
3. Tsubota, M., et al. Aharonov-Bohm effect in charge-density wave loops with inherent temporal current switching. *EPL (Europhysics Letters)* **97**, 57011 (2012).
4. Tucker, J. R. & Feldman, M. J. Quantum detection at millimeter wavelengths. *Rev. Mod. Phys.* **57**, 1055 (1985).
5. Miller Jr., J. H. Qudits employing nonlinear dielectrics. *U.S. Patent Appl. No. 17/981,322*, 2023, filed on behalf of U. Houston (2023).
6. Miller Jr., J. H., et al. J. Hybrid quantum systems for higher temperature quantum information processing. *IEEE Trans. Appl. Superconductivity* **33**, 1700404 (2023).

## Acknowledgements

This research was sponsored by the Army Research Office and was accomplished under Grant Number W911NF-25-1-0071. The views and conclusions contained in this document are those of the authors and should not be interpreted as representing the official policies, either expressed or implied, of the Army Research Office or the U.S. Government. The U.S. Government is authorized to reproduce and distribute reprints for Government purposes notwithstanding any copyright notation herein. Additional support was provided by the Texas Center for Superconductivity.